pH-Responsive Poly(ethylene glycol)/Poly(L-lactide) Supramolecular Micelles Based on Host–Guest Interaction

Zhe Zhang,[†,‡] Qiang Lv,[†,‡] Xiaoye Gao,[†] Li Chen,*[,§] Yue Cao,[†] Shuangjiang Yu,[†] Chaoliang He,*[,†] and Xuesi Chen[†]

[†]Key Laboratory of Polymer Ecomaterials, Changchun Institute of Applied Chemistry, Chinese Academy of Sciences, Changchun 130022, China

[§]Department of Chemistry, Northeast Normal University, Changchun 130024, China

S *Supporting Information*

ABSTRACT: pH-responsive supramolecular amphiphilic micelles based on benzimidazole-terminated poly(ethylene glycol) (PEG-BM) and β-cyclodextrin-modified poly(L-lactide) (CD-PLLA) were developed by exploiting the host–guest interaction between benzimidazole (BM) and β-cyclodextrin (β-CD). The dissociation of the supramolecular micelles was triggered in acidic environments. An antineoplastic drug, doxorubicin (DOX), was loaded into the supramolecular micelles as a model drug. The release of DOX from the supramolecular micelles was clearly accelerated as the pH was reduced from 7.4 to 5.5. The DOX-loaded PEG-BM/CD-PLLA supramolecular micelles displayed an enhanced intracellular drug-release rate in HepG2 cells compared to the pH-insensitive DOX-loaded PEG-b-PLLA counterpart. After intravenous injection into nude mice bearing HepG2 xenografts by the tail vein, the DOX-loaded supramolecular micelles exhibited significantly higher tumor inhibition efficacy and reduced systemic toxicity compared to free DOX. Furthermore, the DOX-loaded supramolecular micelles showed a blood clearance rate markedly lower than that of free DOX and comparable to that of the DOX-loaded PEG-b-PLLA micelles after intravenous injection into rats. Therefore, the pH-responsive PEG-BM/CD-PLLA supramolecular micelles hold potential as a smart nanocarrier for anticancer drug delivery.

KEYWORDS: supramolecular amphiphiles, pH-responsive, host–guest interaction, drug delivery
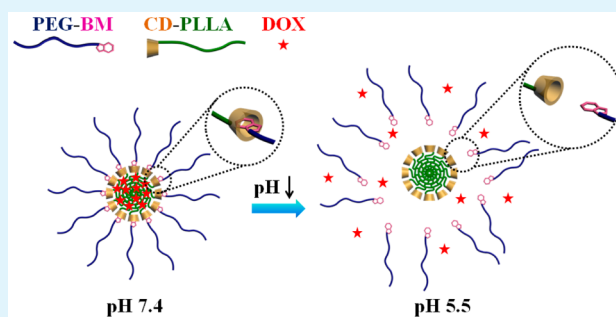
1. INTRODUCTION

Polymeric nanovehicles have received extensive investigation for anticancer drug delivery in the past two decades.[1,2] Core–shell nanocarriers containing a stealthy shell and a hydrophobic core have shown unique advantages for cancer chemotherapy, including improved loading capacity for hydrophobic drugs, prolonged blood circulation, and passive tumor accumulation attributed to the enhanced permeability and retention (EPR) effect.[3] In particular, nanocarriers based on biocompatible and biodegradable polymers have gained considerable attention for their potential in clinical applications.[4] For instance, several biodegradable aliphatic polyesters, such as poly(D,L-lactic acid) (PLA) and biocompatible poly(ethylene glycol) (PEG) have been approved by the U.S. Food and Drug Administration for clinical applications and therefore have been widely studied for drug delivery systems.[5,6] Recently, a paclitaxel- (PTX-) loaded nanoparticle based on PEG-b-PLA diblock copolymer was approved for cancer chemotherapy in South Korea and entered Phase II clinical trails in the United States.[7] Nevertheless, the drug release from the PEG-b-PLA-based nanocarriers is mainly driven by drug diffusion and the degradation of the PLA segments. The PEG-b-PLA nanoparticles are unable to spontaneously release the payloads in response to specific biological microenvironments, leading to limitations in practical therapeutic efficacy. Accordingly, polymeric nanovehicles capable of responding to specific biological triggers have attracted increasing interest as on-demand drug delivery systems in recent years.[8–17]

Nanosized self-assemblies that are formed based on supramolecular interactions, such as host–guest recognition, have received considerable attention because a reversible transition between self-assembly and disassembly can be achieved by adjusting the external environment.[18–20] In particular, supramolecular nanoaggregates that disassemble in response to specific biological stimuli, such as an acidic endosomal/lysosomal environment (pH 5.0–6.5) or intracellular reducing agents, have potential in intracellular drug delivery systems.[21–25] Nevertheless, to date, studies on environment-responsive nanovehicles based on supramolecular copolymers for intelligent drug delivery are still limited. In particular, little

attention has been paid to the in vivo antitumor efficacy and plasma stability of drug-loaded supramolecular block copolymer micelles.

In the present work, a novel pH-responsive supramolecular micelle based on PEG and poly(L-lactide) (PLLA) was developed. The pH-dependent association/dissociation of the complexes formed by benzimidazole- (BM-) terminated PEG (PEG-BM) and β-cyclodextrin- (β-CD-) modified PLLA (CD-PLLA) was revealed by fluorescent measurements (Scheme 1).

Scheme 1. Schematic Illustration of Formation and Triggered Drug Release from DOX-Loaded PEG-BM/CD-PLLA Supramolecular Micelles in Response to the Intracellular Microenvironment
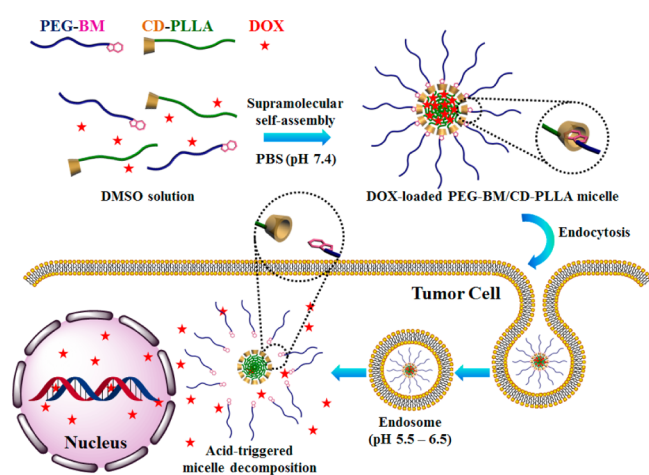
The triggered drug-release behavior of doxorubicin- (DOX-) loaded supramolecular micelles was investigated in an acidic environment, in comparison with that of pH-insensitive DOX-loaded PEG-b-PLLA micelles. To reveal the intracellular release of DOX from the supramolecular micelles, the cellular uptake of the drug-containing micelles and intracellular DOX fluorescence in HepG2 cells were detected by confocal laser scanning microscopy (CLSM) and flow cytometry. Additionally, the cytotoxicities of the DOX-loaded supramolecular micelles against HepG2 and HeLa cells were compared with those of the pH-insensitive DOX-loaded PEG-b-PLLA micelles by MTT assay. Furthermore, the plasma stability of the DOX-loaded supramolecular micelles was monitored after intravenous injection into rats. To further reveal the potential of the DOX-loaded supramolecular micelles as nanovehicles for tumor treatments, the in vivo antitumor efficacy of the DOX-loaded supramolecular micelles was investigated on a nude mice model bearing HepG2 xenografts.

2. EXPERIMENTAL SECTION

2.1. Materials. Methoxypolyethylene glycol (mPEG, M_n = 5 kDa, Aldrich), 2-bromoisobutyryl bromide (BiBB, 98%, Sigma), benzimidazole (BM, 98%, Aldrich), sodium azide (Sigma), propargylamine (98%, Aldrich), propargyl alcohol (99%, Aldrich), N,N,N′,N′,N″-pentamethyldiethylenetriamine (PMDETA, 99%, Aldrich), and N,N-diisopropylethylamine (99.5%, Sigma) were used as received. L-Lactide (LLA) was obtained from PURAC (Gorinchem, The Netherlands) and recrystallized from ethyl acetate before use. Mono-6-deoxy-6-azido-β-cyclodextrin (β-CD-N₃) was prepared according to the method described in the literature.[21,24]

2.2. Synthesis of PEG-BM. mPEG was first modified with 2-bromoisobutyryl bromide (BiBB) (Scheme S1, Supporting Information). Typically, 4.0 g of mPEG (M_n = 5 kDa, 0.8 mmol) was dissolved

in methylene dichloride (50 mL) in a flask under a N₂ atmosphere, after which triethylamine (2.5 mL, 2-fold molar excess relative to BiBB) was added to the flask. Then, 1.0 mL of BiBB (8.0 mmol) was dropped into the flask at 0 °C. After 12 h, the solution was precipitated in a 10-fold excess of diethyl ether. The product was further purified by precipitation in diethyl ether twice to obtain bromide-terminated mPEG (PEG-Br).

PEG-BM was then prepared by the reaction between PEG-Br (0.4 mmol) and benzimidazole (BM, 4 mmol) in the presence of N,N-diisopropylethylamine (4 mmol).[21] The final yield of PEG-BM was 68.1%. ¹H NMR analysis was performed in CDCl₃ (Figure S1, Supporting Information).
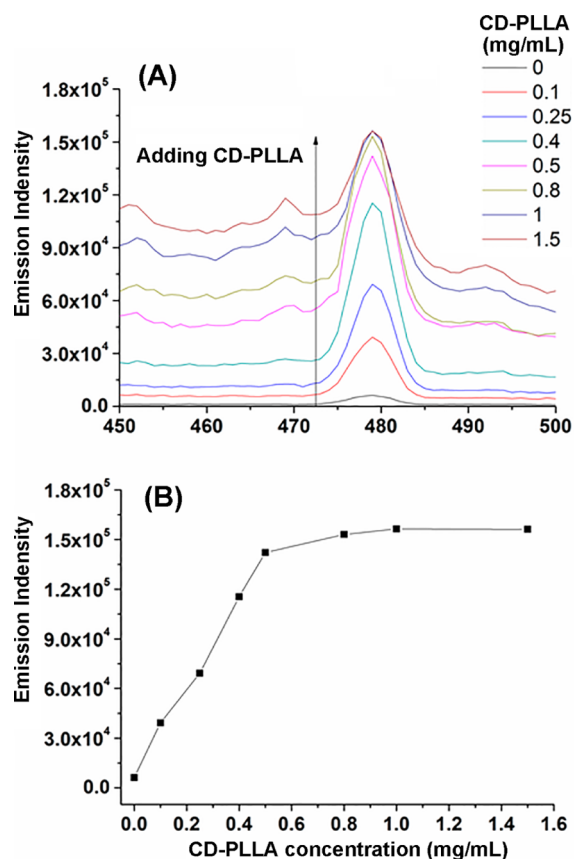
2.3. Synthesis of CD-PLLA. α-Alkyne-terminated PLLA was first obtained by the ring-opening polymerization (ROP) of LLA with propargyl alcohol and stannous octoate [Sn(Oct)₂] as the initiator and catalyst, respectively. Briefly, propargyl alcohol (0.029 mL, 1 mmol), LLA (5 g, 34.7 mmol), and Sn(Oct)₂ (0.014 g, 0.1 mol % relative to LLA) were dissolved in 20 mL of anhydrous toluene in an ampule. The solution was stirred at 120 °C. After 24 h, the solution was poured slowly into excess diethyl ether to gain the crude product. The solid was then purified by being dissolved in trichloromethane and precipitated in diethyl ether three times. After filtration and drying under a vacuum, α-alkyne-terminated PLLA was collected (yield = 72.2%). The molecular weight of the α-alkyne-terminated PLLA was determined to be 4900 g mol⁻¹ by gel permeation chromatography (GPC). The number of repeat units in the PLLA was 68.

CD-PLLA was then prepared by the "click" chemistry between α-alkyne-terminated PLLA and β-CD-N₃ (Scheme S1, Supporting Information). α-Alkyne-terminated PLLA (0.1 mmol), β-CD-N₃ (0.2 mmol), and PMDETA (0.2 mmol) were mixed in anhydrous dimethyl sulfoxide (DMSO, 30 mL). After being degassed through three freeze−thaw cycles, the solution was mixed with CuBr (0.2 mmol) under a N₂ atmosphere. The reaction was allowed to proceed at 60 °C. After 72 h, the product was obtained by dialyzing against deionized water (molecular-weight cutoff of 10 kDa), followed by lyophilization. ¹H NMR analysis of the product was performed in DMSO-d_6 (Figure S2, Supporting Information).

2.4. Synthesis of PEG-b-PLLA Copolymer. Poly(ethylene glycol)-block-poly(L-lactide) (PEG-b-PLLA) diblock copolymer was synthesized by using mPEG as a macroinitiator, as shown in Scheme S2 (Supporting Information). Briefly, mPEG (2 g, 0.4 mmol), LLA (2 g, 13.9 mmol), and Sn(Oct)₂ (0.0056 g, 0.1 mol % relative to LLA) were dissolved in 20 mL of anhydrous toluene in an ampule. The rest of the procedure was similar to that used for the synthesis of α-alkyne-terminated PLLA. The yield of PEG-b-PLLA was 72.2%. The molecular weight was determined to be 9700 g mol⁻¹ according to GPC.
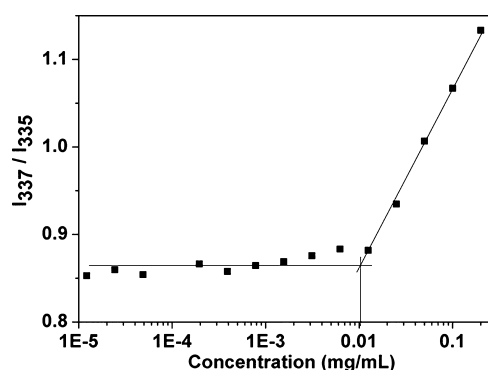
3. RESULTS AND DISCUSSION

Benzimidazole- (BM-) modified mPEG (PEG-BM) was obtained by the reaction between bromide-terminated mPEG and BM (Scheme S1a, Supporting Information). Additionally, β-CD-terminated PLLA (CD-PLLA) was synthesized by the ROP of LLA using propargyl alcohol as an initiator, followed by the alkynyl-azido click reaction (Scheme S1b, Supporting Information). To confirm the successful association of PEG-BM and CD-PLLA, blends of PEG-BM and CD-PLLA with different PEG-BM/CD-PLLA ratios were dissolved in DMSO, and phosphate-buffered saline [PBS, pH 7.4, PBS/DMSO = 9:1 (v/v)] was added dropwise. The fluorescence of the complexes in the mixed solvent was studied. As shown in Figure 1, the PEG-BM concentration was fixed at 0.5 mg/mL, whereas the concentration of CD-PLLA was increased from 0 to 1.5 mg/mL. The pure PEG-BM solution showed typical fluorescence at 478 nm. The emission band was attributed to the anionic state of BM caused by the intermolecular proton transfer between solute and solvent in the excited state.[21,26] As shown in Figure

Figure 1. (A) Fluorescence emission spectra of PEG-BM in aqueous solutions with different CD-PLLA concentrations (λ_{ex} = 240 nm) and (B) emission indensity at 478 nm as a function of CD-PLLA concentration. The concentration of PEG-BM was fixed at 0.5 mg/mL, whereas the concentration of CD-PLLA was increased gradually from 0 to 1.5 mg/mL.

Figure 2. I_{337}/I_{335} intensity ratios from pyrene excitation spectra as a function of concentration of PEG-BM/CD-PLLA supramolecular copolymer in PBS at pH 7.4. The weight ratio of PEG-BM to CD-PLLA was fixed at 1:1.
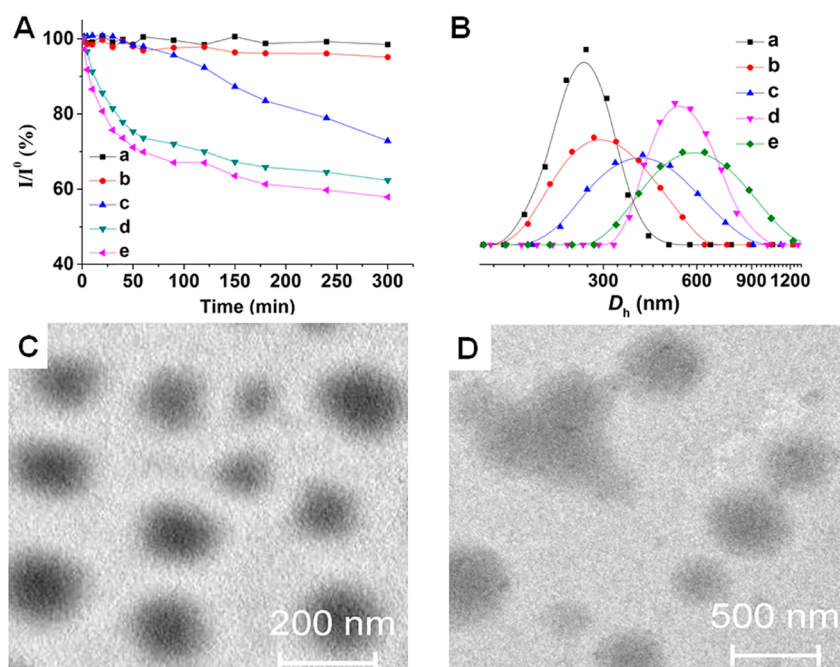
PEG-b-PLLA should be attributed to the stable covalent linkage between PEG and PLLA. The fluorescence test results and aggregation behavior both support the formation of an association between PEG-BM and CD-PLLA.

The dissociation of the PEG-BM/CD-PLLA supramolecular amphiphile in an acidic environment was investigated by detecting the variation in the emission intensity at 478 nm with decreasing pH. As shown in Figure 3A, the fluorescence intensity remained stable at pH 7.4. In contrast, a rapid decrease in the fluorescence intensity was observed as the pH was reduced to 6.5 or less. These results suggest that the PEG-BM/CD-PLLA supermolecular copolymer is stable at physiological pH (pH 7.4) but dissociates in a weakly acidic environment, making this material interesting for triggered drug release within an acidic microenvironment, such as endosomal/lysosomal compartments.

The influence of pH on the size of the supramolecular micelles was studied by dynamic laser scattering (DLS) and transmission electron microscopy (TEM). The hydrodynamic diameter (D_h) of the PEG-BM/CD-PLLA supramolecular micelles was measured at pH 7.4, 6.8, 6.5, 6.0, and 5.5. The D_h values at pH 7.4 and 6.8 were determined to be 272 ± 74 and 314 ± 102 nm, respectively. It is noteworthy that D_h increased markedly as the pH was reduced to 5.5 (402 ± 156, 526 ± 142, and 590 ± 188 nm for pH 6.5, 6.0, and 5.5, respectively) (Figure 3B; Table S1, Supporting Information). For comparison, the D_h value of the micelles of covalently linked PEG-b-PLLA diblock copolymer did not change obviously with changing pH. Additionally, based on TEM measurements, it was found that the PEG-BM/CD-PLLA supramolecular micelles had a spherical morphology with an average diameter of 150−200 nm at pH 7.4 (Figure 3C) and that the particle size also displayed a marked increase at pH 5.5 (Figure 3D). The particle sizes observed by TEM were relatively smaller than those obtained by DLS, likely because of the dehydration and shrinkage of the micelles during the drying of the TEM samples. The pH-sensitive behavior of the supramolecular micelles was obviously revealed. The increase in the particle size under acidic conditions should be due to the formation of aggregates of the hydrophobic PLLA chains after the disassociation of the supramolecular complexes.

To reveal the feasibility of using the supramolecular micelles as nanocarriers for drug delivery, a broad-spectrum anticancer drug, doxorubicin (DOX), was loaded into the PEG-BM/CD-PLLA supramolecular micelles and PEG-b-PLLA micelles. The

1, the increase in CD-PLLA concentration from 0 to 0.5 mg/mL led to a marked increase in the fluorescence intensity of BM. It has been established that the fluorescence intensity of BM increases obviously after association with β-CD.[26] Therefore, the increase in the fluorescence intensity of BM upon the addition of CD-PLLA suggests the formation of a complex between the BM and CD moieties of PEG-BM and CD-PLLA (Scheme S1c, Supporting Information). It is noteworthy that the further increase of the CD-PLLA concentration from 0.8 to 1.5 mg/mL had no obvious influence on the fluorescence intensity of BM. This suggests that the BM moieties were almost fully associated with β-CD of CD-PLLA when the concentration of CD-PLLA was comparable to that of PEG-BM (0.5 mg/mL). Accordingly, the weight ratio of PEG-BM to CD-PLLA in the supramolecular micelles was fixed at 1:1 in the subsequent measurements.

The aggregation behavior of the PEG-BM/CD-PLLA supramolecular amphiphile in aqueous solution was studied by fluorescence. As shown in Figure 2, at pH 7.4, the critical micellization concentration (CMC) of the PEG-BM/CD-PLLA supramolecular amphiphile was determined to be 10.1 μg/mL. To demonstrate the aggregation properties of PEG-BM/CD-PLLA, a PEG-b-PLLA diblock copolymer containing similar PEG and PLLA block lengths was synthesized, and the CMC of PEG-b-PLLA was measured for comparison. The CMC of PEG-b-PLLA was found to be 1.4 μg/mL (Figure S4, Supporting Information). The relatively lower CMC for

Figure 3. (A) Normalized fluorescence emission intensity (λ_{em} = 478 nm) of PEG-BM/CD-PLLA copolymer in PBS solutions (1 mg/mL) as a function of time and (B) hydrodynamic diameters (D_h) of PEG-BM/CD-PLLA in PBS (0.1 mg/mL) at different pH values: (a) pH 7.4, (b) pH 6.8, (c) pH 6.5, (d) pH 6.0, (e) pH 5.5. (C,D) TEM micrographs of PEG-BM/CD-PLLA solutions (0.1 mg/mL) formed at pH (C) 7.4 and (D) 5.5.

drug loading contents (DLCs) of the DOX-loaded PEG-BM/CD-PLLA and PEG-*b*-PLLA micelles were 4.6% and 5.5%, respectively (Table S2, Supporting Information). The in vitro release behaviors of DOX from the DOX-loaded PEG-BM/CD-PLLA and PEG-*b*-PLLA micelles were investigated at pH 7.4, 6.5, and 5.5. As shown in Figure 4, the release of DOX
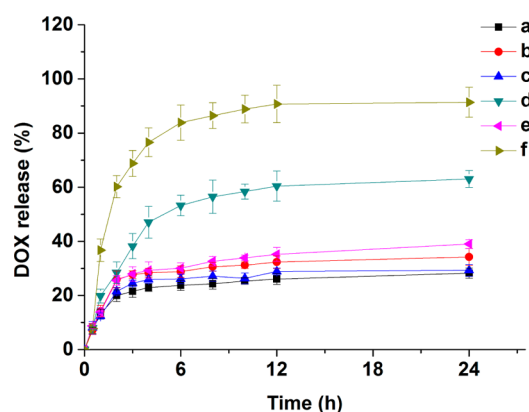
Figure 4. In vitro DOX release profiles of DOX-loaded micelles in PBS at 37 °C and different pH values: (a,c,e) DOX-loaded PEG-*b*-PLLA and (b,d,f) DOX-loaded PEG-BM/CD-PLLA at pH (a,b) 7.4, (c,d) 6.5, and (e,f) 5.5.

from the PEG-BM/CD-PLLA micelles was suppressed at pH 7.4, and only about 30% of the DOX was released within 24 h. In contrast, the DOX release was markedly accelerated at pH 6.5 and pH 5.5, and ~90% of the DOX was released from the DOX-loaded PEG-BM/CD-PLLA supramolecular micelles in 24 h at pH 5.5. It is noteworthy that the drug release from the pH-insensitive DOX-loaded PEG-*b*-PLLA micelles was not obviously influenced by reducing the pH from 7.4 to 5.5 (Figure 4). Hence, the acid-triggered drug release of the supramolecular micelles can be reasonably attributed to the

acid-induced decomposition of the supramolecular micelles caused by the decomplexation of the BM/CD complexes.

To investigate the potential of the supramolecular micelles for intelligent drug release in response to a biological environment, the cellular uptake and intracellular drug release of the DOX-loaded PEG-BM/CD-PLLA and PEG-*b*-PLLA micelles in HepG2 cells were tested by confocal laser scanning microscopy (CLSM) and flow cytometry. Based on the CLSM and flow cytometry results (Figures 5 and 6, respectively), after incubation for 3 h, an obviously higher DOX fluorescence intensity was detected in the cells incubated with DOX-loaded PEG-BM/CD-PLLA supramolecular micelles than in those incubated with the pH-insensitive DOX-loaded PEG-*b*-PLA counterpart. These results clearly suggest a faster intracellular drug-release process for the pH-responsive supramolecular micelles, likely resulting from acid-triggered micelle dissociation in the acidic endosomal/lysosomal compartments (Scheme 1).

Moreover, the cytotoxicities of the DOX-loaded PEG-BM/CD-PLLA and PEG-*b*-PLLA micelles against HepG2 and HeLa cells were evaluated by MTT assay. Both the bare PEG-BM/CD-PLLA and PEG-*b*-PLLA micelles exhibited no detectable cytotoxicities against HepG2 and HeLa cells (Figure S5, Supporting Information). Notably, it was found that the pH-responsive DOX-loaded supramolecular micelles displayed enhanced cytotoxicities against both HepG2 and HeLa cells, compared to the DOX-loaded pH-insensitive PEG-*b*-PLLA micelles (Figures 7 and S6, Supporting Information). The IC_{50} values of free DOX and DOX-loaded PEG-BM/CD-PLLA and PEG-*b*-PLLA micelles against HepG2 and HeLa cells after incubation for 72 h are listed in Table S3 (Supporting Information). The results further confirm the rapid intracellular drug-release process of the DOX-loaded supramolecular micelles, providing an increased intracellular drug dose and higher cytotoxicity.[27]

Furthermore, the in vivo antitumor efficacy of the DOX-loaded supramolecular micelles was investigated on BALB/c
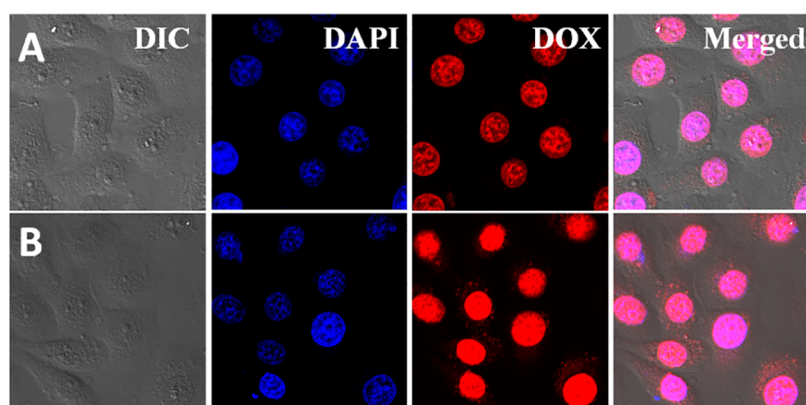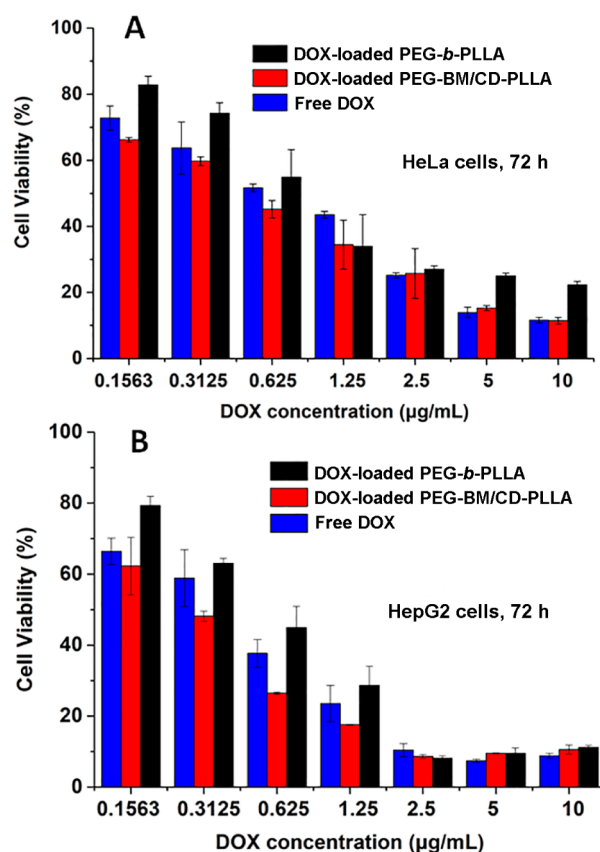
Figure 5. Representative CLSM images of HepG2 cells after incubation with (A) DOX-loaded PEG-*b*-PLLA micelles and (B) DOX-loaded PEG-BM/CD-PLLA supramolecular micelles for 3 h. For each panel, the images from left to right show differential interference contrast (DIC) image, cell nuclei stained by DAPI (blue), DOX fluorescence in cells (red), and overlays of the three images, respectively.
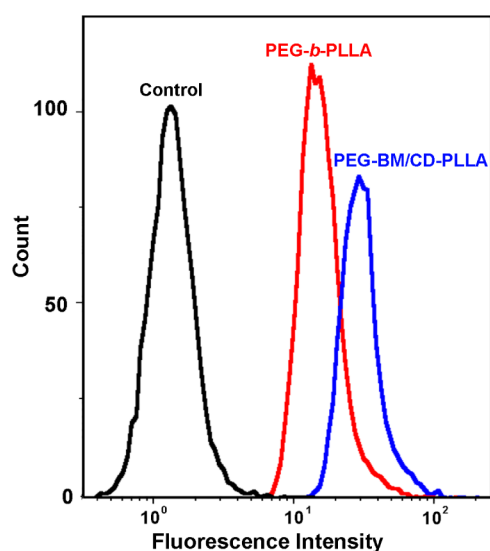

Figure 6. Flow cytometric profiles of HepG2 cells after incubation with DOX-loaded PEG-BM/CD-PLLA and PEG-*b*-PLLA micelles for 3 h.

Figure 7. Cytotoxicities of DOX-loaded PEG-BM/CD-PLLA supramolecular micelles, DOX-loaded PEG-*b*-PLLA micelles, and free DOX against (A) HeLa and (B) HepG2 cells after incubation for 72 h.

nude mice bearing HepG2 xenografts (sections S1.6 and S1.7 of the Supporting Information).[28] The tumor-bearing mice were treated with free DOX, DOX-loaded PEG-*b*-PLLA micelles, or DOX-loaded PEG-BM/CD-PLLA micelles by tail-vein injection of the drug formulations at days 0, 3, and 6. As shown in Figure 8, compared to the control group treated with PBS, the treatments with DOX-loaded micelles or free DOX led to the obvious suppression of tumor growth. Notably, the pH-responsive DOX-loaded PEG-BM/CD-PLLA micelles exhibited significantly enhanced tumor inhibition efficacy compared to free DOX. The higher tumor inhibition efficacy of the DOX-loaded supramolecular micelles compared to free DOX can be attributed to the improved tumor accumulation of DOX and fast intracellular drug release. It was observed that the in vivo antitumor efficacy of the DOX-loaded supramolecular micelles was slightly higher than that of the DOX-loaded PEG-*b*-PLLA micelles ($P > 0.05$). No statistically significant difference between the in vivo tumor suppression efficacies of the DOX-loaded PEG-BM/CD-PLLA supramolecular micelles and DOX-loaded PEG-*b*-PLLA micelles was observed. This might be due to the relatively lower stability of the supramolecular micelles compared to the covalently linked

block copolymer micelles in blood circulation, even though the DOX-loaded supramolecular micelles showed higher antiproliferation efficacy against HepG2 cells in vitro. Moreover, the treatments with the DOX-loaded PEG-*b*-PLLA and PEG-BM/CD-PLLA micelles caused no obvious body loss after 16 days of treatment (Figure 8B). In contrast, the treatments with free DOX caused marked body loss of the mice, implying severe systemic adverse effects of free DOX. The results indicate that the DOX-loaded micelles caused a lower systemic toxicity than free DOX at comparable dosage. After 16 days of treatment, all of the mice were sacrificed. The tumors from each treatment
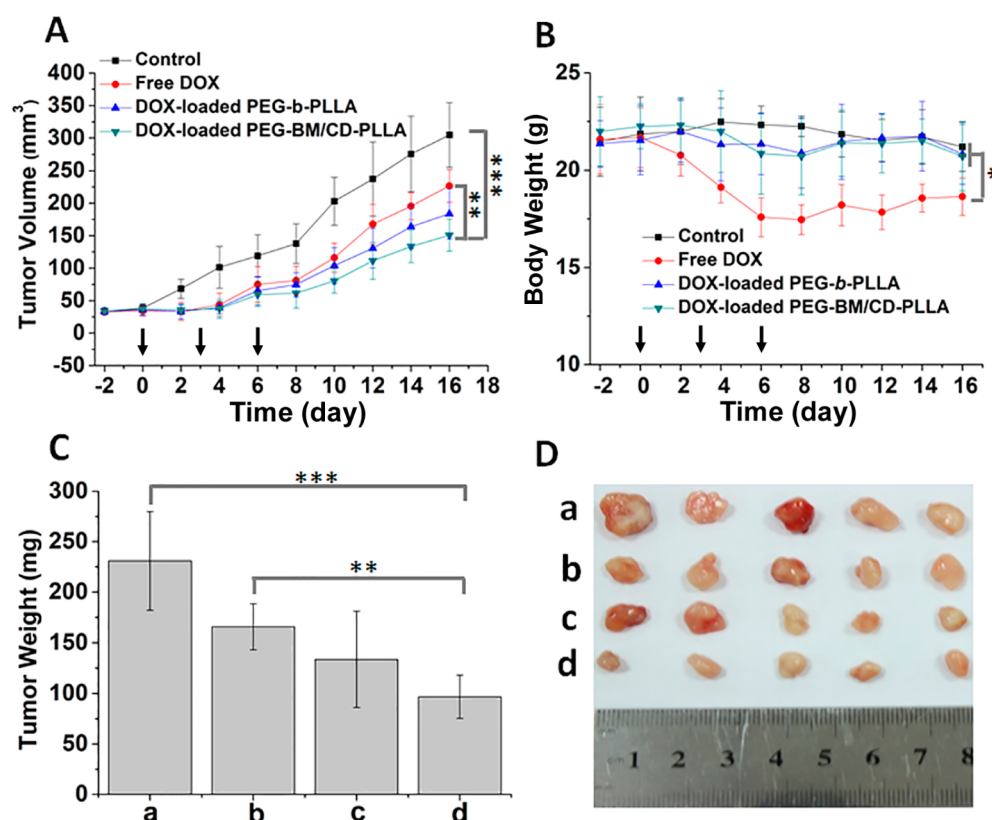
Figure 8. In vivo antitumor efficacies after tail-vein injection of PBS (control), free DOX, DOX-loaded PEG-*b*-PLLA, and DOX-loaded PEG-BM/CD-PLLA into male BALB/c nude mice bearing HepG2 xenografts. (A) Variation profiles of tumor volumes. (B) Body weights of tumor-bearing mice. (C) Tumor weights after the mice were sacrificed at day 16 of treatment. (D) Photograph of the tumors after the mice were sacrificed at day 16: (a) control, (b) free DOX, (c) DOX-loaded PEG-*b*-PLLA, and (d) DOX-loaded PEG-BM/CD-PLLA. Arrows indicate the treatment times. Data given as mean ± SD ($n = 5$) (*, $p < 0.05$; **, $p < 0.01$; ***, $p < 0.001$).

group were removed and weighed (Figure 8C,D). The differences in tumor weight were consistent with the tumor volumes. Therefore, the results indicate that the encapsulation of DOX in the PEG-BM/CD-PLLA supramolecular micelles led to enhanced antitumor efficacy and reduced systemic toxicity.

The in vivo distribution of the micelles was further studied by ex vivo DOX fluorescence imaging. As shown in Figure 9A, photographs of the isolated organs, including heart, liver, spleen, lung, and kidney, as well as tumor masses were obtained 3 h after tail-vein injection of different formulations in the nude mice bearing HepG2 xenografts.[29] It was found that the liver and kidney of the mice treated with free DOX exhibited stronger DOX fluorescence, indicating higher accumulation of DOX. However, obviously weaker DOX fluorescence in the liver and kidney of the mice treated with DOX-loaded PEG-*b*-PLLA and PEG-BM/CD-PLLA micelles was observed. These results suggest that the DOX-loaded micelles showed lower drug accumulation in the liver and kidney than free DOX.

To investigate the plasma stability of the DOX-loaded supramolecular micelles in vivo, the plasma pharmacokinetics of free DOX and DOX-loaded PEG-*b*-PLLA and PEG-BM/CD-PLLA micelles were measured after intravenous administration to Wistar rats. As shown in Figure 9B, the decline in the plasma DOX concentration after treatments with free DOX or DOX-loaded micelles occurred in an exponential manner. The DOX-loaded PEG-BM/CD-PLLA supramolecular micelles displayed slightly lower plasma stability than the DOX-loaded PEG-*b*-PLLA micelles. This should be due to the fact that

supramolecular interactions are relatively weaker than covalent bonds. It is noteworthy that the DOX-loaded PEG-BM/CD-PLLA micelles displayed significantly prolonged blood retention compared to free DOX. This indicates an effective retardation in blood clearance and a prolonged blood circulation time of the drug-loaded supramolecular micelles, which could promote the tumor accumulation of DOX through the EPR effect during tumor treatments.

4. CONCLUSIONS

A type of pH-responsive PEG-BM/CD-PLLA supramolecular micelles was developed based on host−guest recognition. The acid-triggered dissociation of the supramolecular self-assemblies was revealed. The release of DOX from the supramolecular micelles was enhanced markedly as the pH was decreased from 7.4 to 5.5, in contrast to the lack of any obvious change in the drug-release behavior of pH-insensitive DOX-loaded PEG-*b*-PLLA micelles. The faster intracellular DOX release and enhanced cytotoxicities of the DOX-loaded supramolecular micelles compared to the pH-insensitive PEG-*b*-PLLA micelles further confirmed the triggered intracellular drug-release process. Moreover, in vivo tests demonstrated that the DOX-loaded supramolecular micelles exhibited an enhanced blood circulation time compared to free DOX after intravenous injection into rats. Following tail-vein injection into nude mice bearing HepG2 xenografts, the DOX-loaded supramolecular micelles displayed significantly enhanced antitumor efficacy and reduced toxic side effects compared to free DOX. Therefore,
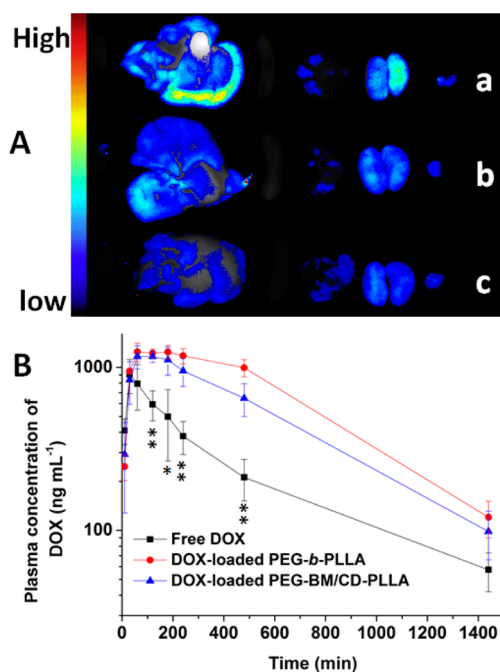
Figure 9. (A) Ex vivo DOX fluorescence images for the drug distributions in the major organs (heart, liver, spleen, lungs, and kidneys) and tumor of nude mice bearing HepG2 tumor after tail-vein injection of (a) free DOX, (b) DOX-loaded PEG-b-PLLA micelles, and (c) DOX-loaded PEG-BM/CD-PLLA micelles for 3 h. (B) In vivo plasma DOX concentrations after tail-vein injection of free DOX, DOX-loaded PEG-b-PLLA micelles, and DOX-loaded PEG-BM/CD-PLLA micelles in Wistar rats. Data are presented as a mean with standard deviation ($n = 3$) (*, $p < 0.05$; **, $p < 0.01$).

the pH-responsive supramolecular micelles might hold potential as intelligent nanocarriers for anticancer drug delivery.

ASSOCIATED CONTENT

Ⓢ Supporting Information

Additional experimental methods, characterization data, in vitro drug loading and release tests, CLSM observations, flow cytometric analysis, cytotoxicity assay, and in vivo antitumor efficacy and plasma drug concentration tests. This material is available free of charge via the Internet at http://pubs.acs.org.

AUTHOR INFORMATION

Corresponding Authors
*E-mail: clhe@ciac.ac.cn. Tel./Fax: +86 431 85262116 (C.H.).
*E-mail: chenl686@nenu.edu.cn (L.C.).

Author Contributions
‡Z.Z. and Q.L. contributed equally to this work.

Notes
The authors declare no competing financial interest.

ACKNOWLEDGMENTS

REFERENCES

(1) Kataoka, K.; Harada, A.; Nagasaki, Y. Block Copolymer Micelles for Drug Delivery: Design, Characterization and Biological Significance. *Adv. Drug Delivery Rev.* **2001**, *47*, 113−131.

(2) Elsabahy, M.; Wooley, K. L. Design of Polymeric Nanoparticles for Biomedical Delivery Applications. *Chem. Soc. Rev.* **2012**, *41*, 2545−2561.

(3) Maeda, H. The Enhanced Permeability and Retention (EPR) Effect in Tumor Vasculature: The Key Role of Tumor-Selective Macromolecular Drug Targeting. *Adv. Enzyme Regul.* **2001**, *41*, 189−207.

(4) Tian, Y.; Tang, Z.; Zhuang, X.; Chen, X.; Jing, X. Biodegradable Synthetic Polymers: Preparation, Functionalization and Biomedical Application. *Prog. Polym. Sci.* **2012**, *37*, 237−280.

(5) Oh, J. K. Polylactide (PLA)-Based Amphiphilic Block Copolymers: Synthesis, Self-Assembly, and Biomedical Applications. *Soft Matter* **2011**, *7*, 5096−5108.

(6) Inkinen, S.; Hakkarainen, M.; Albertsson, A. C.; Sodergard, A. From Lactic Acid to Poly(lactic acid) (PLA): Characterization and Analysis of PLA and Its Precursors. *Biomacromolecules* **2011**, *12*, 523−532.

(7) Deng, C.; Jiang, Y.; Cheng, R.; Meng, F.; Zhong, Z. Biodegradable Polymeric Micelles for Targeted and Controlled Anticancer Drug Delivery: Promises, Progress and Prospects. *Nano Today* **2012**, *7*, 467−480.

(8) Bae, Y.; Kataoka, K. Intelligent Polymeric Micelles from Functional Poly(ethylene glycol)−Poly(amino acid) Block Copolymers. *Adv. Drug Delivery Rev.* **2009**, *61*, 768−784.

(9) Cheng, R.; Feng, F.; Meng, F.; Deng, C.; Feijen, J.; Zhong, Z. Glutathione-Responsive Nano-Vehicles as a Promising Platform for Targeted Intracellular Drug and Gene Gelivery. *J. Controlled Release* **2011**, *152*, 2−12.

(10) He, C.; Zhuang, X.; Tang, Z.; Tian, H.; Chen, X. Stimuli-Sensitive Synthetic Polypeptide-Based Materials for Drug and Gene Delivery. *Adv. Healthcare Mater.* **2012**, *1*, 48−78.

(11) Ge, Z.; Liu, S. Functional Block Copolymer Assemblies Responsive to Tumor and Intracellular Microenvironments for Site-Specific Drug Delivery and Enhanced Imaging Performance. *Chem. Soc. Rev.* **2013**, *42*, 7289−7325.

(12) Li, Y.; Gao, G. H.; Lee, D. S. Stimulus-Sensitive Polymeric Nanoparticles and Their Applications as Drug and Gene Carriers. *Adv. Healthcare Mater.* **2013**, *2*, 388−417.

(13) Dai, J.; Lin, S.; Cheng, D.; Zou, S.; Shuai, X. Interlayer-Crosslinked Micelle with Partially Hydrated Core Showing Reduction and pH Dual Sensitivity for Pinpointed Intracellular Drug Release. *Angew. Chem., Int. Ed.* **2011**, *50*, 9404−9408.

(14) Du, J. Z.; Du, X. J.; Mao, C. Q.; Wang, J. Tailor-Made Dual pH-Sensitive Polymer−Doxorubicin Nanoparticles for Efficient Anticancer Drug Delivery. *J. Am. Chem. Soc.* **2011**, *133*, 17560−17563.

(15) Li, Z. Y.; Liu, Y.; Wang, X. Q.; Liu, L. H.; Hu, J. J.; Luo, G. F.; Chen, W. H.; Rong, L.; Zhang, X. Z. One-Pot Construction of Functional Mesoporous Silica Nanoparticles for the Tumor-Acidity-Activated Synergistic Chemotherapy of Glioblastoma. *ACS Appl. Mater. Interfaces* **2013**, *5*, 7995−8001.

(16) Ding, M.; Song, N.; He, X.; Li, J.; Zhou, L.; Tan, H.; Fu, Q.; Gu, Q. Toward the Next-Generation Nanomedicines. Design of Multifunctional Multiblock Polyurethanes for Effective Cancer Treatment. *ACS Nano* **2013**, *7*, 1918−1928.

(17) Sui, M.; Liu, W.; Shen, Y. Nuclear Drug Delivery for Cancer Chemotherapy. *J. Controlled Release* **2011**, *155*, 227−236.

(18) Zhang, X.; Wang, C. Supramolecular Amphiphiles. *Chem. Soc. Rev.* **2011**, *40*, 94−101.

(19) Schmit, B. V. K. J.; Hetzer, M.; Ritter, H.; Barner-Kowollik, C. Complex Macromolecular Architecture Design via Cyclodextrin Host−Guest Complexes. *Prog. Polym. Sci.* **2014**, *39*, 235−249.

(20) Li, J.; Loh, X. J. Cyclodextrin-Based Supramolecular Architectures: Syntheses, Structures, and Applications for Drug and Gene Delivery. *Adv. Drug Delivery Rev.* **2008**, *60*, 1000−1017.

(21) Zhang, Z.; Ding, J.; Chen, X.; Xiao, C.; He, C.; Zhuang, X.; Chen, L.; Chen, X. Intracellular pH-Sensitive Supramolecular Amphiphiles Based on Host−Guest Recognition between Benzimidazole and β-Cyclodextrin as Potential Drug Delivery Vehicles. *Polym. Chem.* **2013**, *4*, 3265−3271.

(22) Zhao, J.; Chen, C.; Li, D.; Liu, X.; Wang, H.; Jin, Q.; Ji, J. Biocompatible and Biodegradable Supramolecular Assemblies Formed with Cucurbit[8]uril as a Smart Platform for Reduction-Triggered Release of Doxorubicin. *Polym. Chem.* **2014**, *5*, 1843−1847.

(23) Sambe, L.; Stoffelbach, F.; Poltorak, K.; Lyskawa, J.; Malfait, A.; Bria, M.; Cooke, G.; Woisel, P. Elaboration of Thermoresponsive Supramolecular Diblock Copolymers in Water from Complementary CBPQT^{4+} and TTF End-Functionalized Polymers. *Macromol. Rapid Commun.* **2014**, *35*, 498−504.

(24) Huan, X.; Wang, D.; Dong, R.; Tu, C.; Zhu, B.; Yan, D.; Zhu, X. Supramolecular ABC Miktoarm Star Terpolymer Based on Host−Guest Inclusion Complexation. *Macromolecules* **2012**, *45*, 5941−5947.

(25) Yao, X.; Chen, L.; Chen, X.; Zhang, Z.; Zheng, H.; He, C.; Zhang, J.; Chen, X. Intracellular pH-Sensitive Metallo-Supramolecular Nanogels for Anticancer Drug Delivery. *ACS Appl. Mater. Interfaces* **2014**, *6*, 7816−7822.

(26) Chowdhury, P.; Adhikary, T. P.; Chakravorti, S. Effect of Additives on the Photophysics of 2-Acetyl Benzimidazole and 2-Benzoyl Benzimidazole Encapsulated in Cyclodextrin Cavity. *J. Photochem. Photobiol. A* **2005**, *173*, 279−286.

(27) Lee, E. S.; Shin, H. J.; Na, K.; Bae, Y. H. Poly(L-histidine)−PEG Block Copolymer Micelles and pH-Induced Destabilization. *J. Controlled Release* **2003**, *90*, 363−374.

(28) Li, M.; Tang, Z.; Lv, S.; Song, W.; Hong, H.; Jing, X.; Zhang, Y.; Chen, X. Cisplatin Crosslinked pH-Sensitive Nanoparticles for Efficient Delivery of Doxorubicin. *Biomaterials* **2014**, *35*, 3851−3864.

(29) Hu, X.; Guan, X.; Li, J.; Pei, Q.; Liu, M.; Xie, Z.; Jing, X. Hybrid Polymer Micelles Capable of cRGD Targeting and pH-Triggered Surface Charge Conversion for Tumor Selective Accumulation and Promoted Uptake. *Chem. Commun.* **2014**, *50*, 9188−9191.